Desalination and Water Treatment
www.deswater.com
doi: 10.5004/dwt.2022.28709

268 (2022) 153–169
August

Assessment of hydrochemical properties of groundwater in the alluvial aquifer of the arid zone of the Igli Region, South-West of Algeria

Houria Abdelbaki[a,*], Abdeldjalil Belkendil[b], Abdelhak Maazouzi[a], Abderrahmane Mekkaoui[c]

[a]*Laboratory of Chemistry and Environmental Science, University of Béchar, Algeria, email: houriaabdelbaki@yahoo.com (H. Abdelbaki)*
[b]*Laboratory 60: Water Resources Valorization, Science and Technology Faculty, University of Tlemcen, Tlemcen, Algeria, email: algeria7002@gmail.com (A. Belkendil)*
[c]*FIMAS Laboratory, University Tahri Mohamed, Béchar, Algeria, email: mekaouidh15@gmail.com (A. Mekkaoui)*

Received 4 January 2022; Accepted 12 July 2022

ABSTRACT

During the last decades, Algeria has been subjected to an intense drought that has particularly affected the southern region. Consequently, groundwater use has proven to be more than an inevitable necessity. The region of Igli, an oasis located in southwestern Algeria at the confluence of the Zousfana and Guir wadis, is located 160 km south of the capital city of Béchar. This region is part of the ancient Saharan platform and has always experienced water quantity and quality problems. The latter situation is only the result of population growth, expansion of the industrial sector, and agricultural development. This study aims to evaluate the infero-flow aquifer of the Igli Region and the impact of natural and anthropogenic factors on groundwater quality in this region. Samples were collected from 16 groundwater points in the study area. The analytical results show that slight alkalinity characterizes the groundwater with an average (pH = 7.59) value. High conductivity values represent high mineralization due to an ionic reaction between water and host rocks in the dissolution of minerals. In addition, the human factor is responsible for the discharge of untreated urban wastewater and septic tanks arbitrarily located in the study area.

Keywords: Cluster analysis; Irrigation adaptation; Infero-flux; Salinity; Igli Oasis; Piper diagram

1. Introduction

Worldwide, water quality and quantity are under threat [1]. Most countries are experiencing significant water shortages, especially in arid and semi-arid regions [2]. Despite new dams and desalination, Algeria will have a water deficit of 1 billion m^3 by 2025 [3]. To cope with the growth in water supply for agricultural and urban purposes in the Saharan oasis, significant mobilization of water resources from deep aquifers (Continental Intercalative and Complex Terminal Aquifers) has been necessary [4,5]. However, the considerable increase in flow rates and the haphazard use of water resources have resulted in wasteful use, resulting in huge amounts of excess water, which has caused surface water tables to rise and promoted environmental degradation [6].

Saharan oases owe their survival and success to the considerable availability of underground water reserves in an environment as harsh and hostile as the Sahara. For a correct groundwater study, attention must be paid to quantitative and qualitative aspects. pH is an important parameter to characterize the acid–base properties of water and the quality of water for drinking uses; permissible limits for pH in drinking water range from 6.5 to 8.5 [7]. pH values

* Corresponding author.

in drinking water outside of the allowable values can cause eye irritation, skin irritation, and gastrointestinal upset [8]. Electrical conductivity is the parameter that indicates the ability of water to transfer electrical current. The World Health Organization has confirmed that electrical conductivity (EC) values in water must be less than 1,500 μS/cm to be potable [7]. Total dissolved solids (TDS) values are considered a basic indicator of whether the groundwater studied is suitable for drinking and irrigation, especially water recorded with high TDS values.

According to the World Health Organization, the allowable value of TDS should not exceed 1,000 mg/L to avoid consumer health issues [9]. Calcium Ca^{2+} and magnesium Mg^{2+} are the most important cations in the physico-chemical parameters of groundwater. According to the standards adopted by the World Health Organization, the maximum allowable values for calcium should not exceed 200 mg/L. As for magnesium, no maximum value has been set, but the imbalance in the values of these elements can lead to health damage such as hypertension diseases, bone problems, cardiac arrhythmias, and many other symptoms of excess or deficiency of calcium and magnesium in drinking water [10]. Researchers have classified sodium Na^{+} as one of the most abundant elements in natural water [11]. Through experiments, it has become clear that exceeding permissible sodium levels contribute to many diseases, including blood pressure, arteriosclerosis, and hyperosmolarity [12].

In addition, higher sodium values negatively affect agricultural land and the quality of crops by damaging the soil [13]. The maximum value for sodium has been set at 200 mg/L [7]. Chloride Cl^{-} is an important anion in natural waters. The recommended chloride values for drinking water should be less than 250 mg/L. Excessive amounts of chloride in water are generally estimated to indicate groundwater contamination and pollution [14]. Nitrate values are an important anion that measures groundwater contamination rates from a source of possible pollution sources (wastewater, excessive fertilizer use, etc.). The desirable limit of NO_3^- in drinking water should not exceed 50 mg/L [7]. Consumption of water with nitrate values above this threshold can negatively affect the human body [15].

This study conducts a physico-chemical characterization of groundwater in the alluvial aquifer of the Igli Region to determine the degree of compatibility of these waters with major human and agricultural activities in the study area. Many scientists and researchers have confirmed that the study of the change in the concentration of major ions in spatial and temporal terms may be sufficient to perceive the characteristics and processes controlling the water chemistry [16–18]. During this study, we used the graphical representation of the concentration of the studied water samples to know the spatial effect of the location of the samples on the characteristics of the water chemistry according to the geological diversity of each part of the study area [19,20]. Numerous graphs were used, such as the Piper diagram, to determine the chemical facies of each sample and the interrelationships between them through the use of cluster analysis, which classifies these samples into small interconnected groups based on location [21–23]. Principal component analysis (PCA) was applied to the sampled chemical parameters to better understand groundwater hydrochemistry [24,25].

2. Study area

The territory of the commune of Igli is located in the center of the province of Béchar, in the South-West of Algeria (between 2°10′ and 2°20′ West and between 30°20′ and 30°35′ North). Its capital is 153 km south of the city of Béchar, 63 km south of Taghit, and 75 km north of Béni Abbès, two famous tourist sites in the region. Igli is the point where the rivers Guir and Zousfana meet, thus becoming the Oued Saoura (Fig. 1). The region of Igli is under the influence of a hyperarid climate with a hot and dry summer and very cold winter and precipitation that does not exceed 83 mm/y. In May 2021, 8,180 people were working mainly in agriculture and livestock.

2.1. Geological setting

The study area belongs to the Saharan platform [26]; it is characterized by a carboniferous bedrock overlain by continental deposits of the Mio-Plio-Quaternary tabular age [27]. The Carboniferous formations dip monoclinally to the South-West with a dip of 10°–30° and consist of various deposits, ranging from Upper Visian to Namurian (Fig. 2). Overall, the structure of the study area is related to the tectonics of the Ougarta Mountains, the latter being characterized by "A flexible or plicative tectonic and a brittle tectonic" [28]. The studied area comprises various sediments belonging to the Carboniferous on the litho-stratigraphic level. The geological map of Béni Abbès, drawn by [29], shows the outcrops encountered in the areas studied. The lithological succession is Carbonifer, Mio-Pliocene (Neogene), and Quaternary.

2.2. Hydrogeological framework

From a hydrogeological point of view, two aquifers can be distinguished. The lower aquifer includes all the carboniferous formations allowing the presence of water in the formations constituted by the carboniferous series called, according to the local jargon [29]: El Hariga (750 m), Akacha-Mazzer (250 m), Boulmane (750 m), Harrez (200 m), Igli (150 m) and Taouerta series (250 m). The upper aquifer is complex in detail. It contains the western aquifer of the Grand Erg and the lower terraces of the Saoura. Note that the works concerned by this study are located in the latter [30–34]. According to Roche [31] (Fig. 3), there are two plausible possibilities for recharging the water table in the Grand Erg Occidental: rainwater infiltration and the legacy of the humid phases of the Quaternary, particularly the last Neolithic phase.

2.3. Methodology

A sampling network was designed to collect data representative of the geographic variation of potable groundwater in the region. This network consists of 16 wells that are scattered around the research site. In general, the depth of the sampling wells varies between 10 and 15 m.

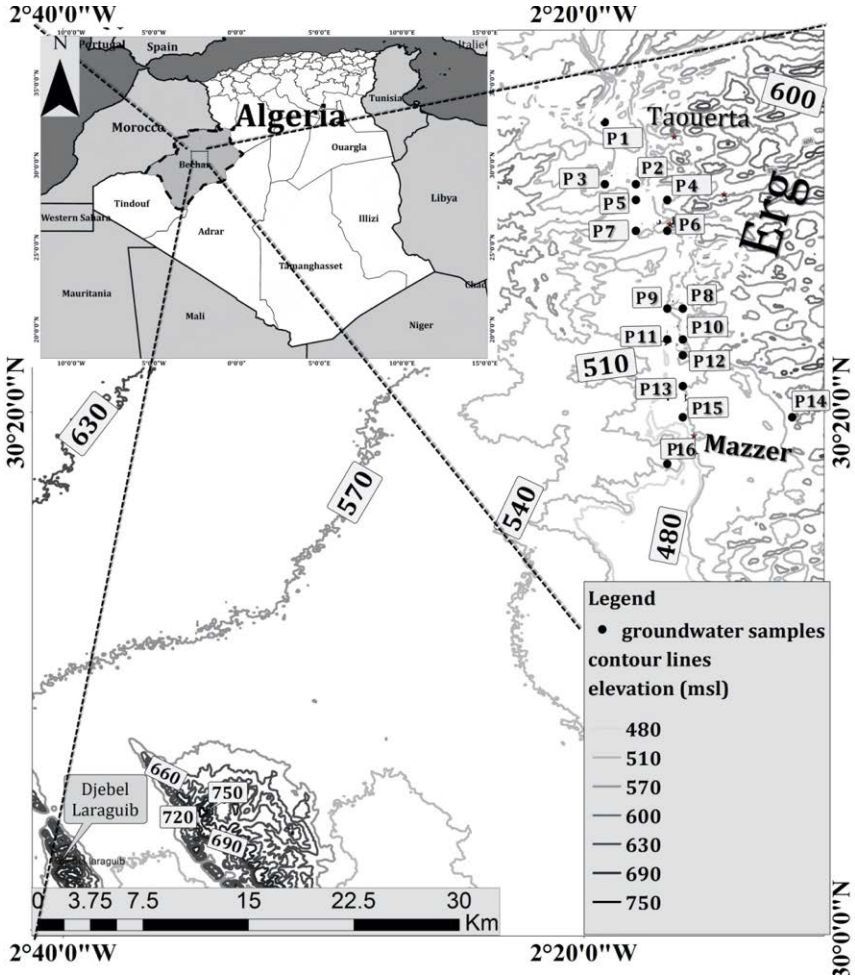

Fig. 1. Location of the study area.

The campaigns took place in October of the year 2018. A volume of 1.5 L intended for physico-chemical analysis is taken in polyethylene bottles made at the National Agency of Water Resources (ANRH) of Adrar. The sampling bottles were transported to the laboratory in a cooler at a low temperature (4°C). The physico-chemical parameters (temperature, conductivity, pH, and salinity) were measured in situ using a multiparameter (Consort 861) with a tolerance of 2%. In the laboratory, the following dosing procedures were applied:

- Potentiometric method (Consort 861) for pH, salinity, HCO_3 and EC conductivity;
- The apparent TDS values were estimated using the following relationship: Conductivity;
- TDS = K × EC (at 25°C), the TDS/EC ratio (k-value) for natural water is between 0.55 and 0.75 [35];
- The volumetric method is applied to the quantitative analysis of calcium and magnesium. The calcium and magnesium contents of the samples are determined by complexometric titration, with the disodium salt of ethylenediaminetetraacetic acid (EDTA); NFT90-003;
- The measurement of nitrates is done by the potentiometric method (HI 121) using a specific electrode;
- Spectrophotometry was used to determine sulfates by precipitating sulfates as barium sulfate with barium chloride. The resulting very fine precipitate was stabilized with gelatin. A turbidimetric measurement at a wavelength of 495 nm is performed on the turbidity;
- Flame spectrophotometry with a wavelength of 495 nm to determine sodium and potassium content.

3. Results and discussion

3.1. Physical parameters

Table 1 lists the analytical results of the groundwater sample investigation for the 2018 sampling campaign. The *hydrogen potential* (pH) ranges from 7.02 to 8.83; this may indicate that all of our samples meet the World Health Organization standards [7] and that the groundwater in this area is alkaline to a minor degree (pH > 7.0). This result can be explained by the influence of infiltration from the surface [36].

The EC values range from 547 to 14,990 μS/cm. Thus, more than 87.5% of the water samples exceed the recommended 1,500 μS/cm standard [7]. They were not allowed

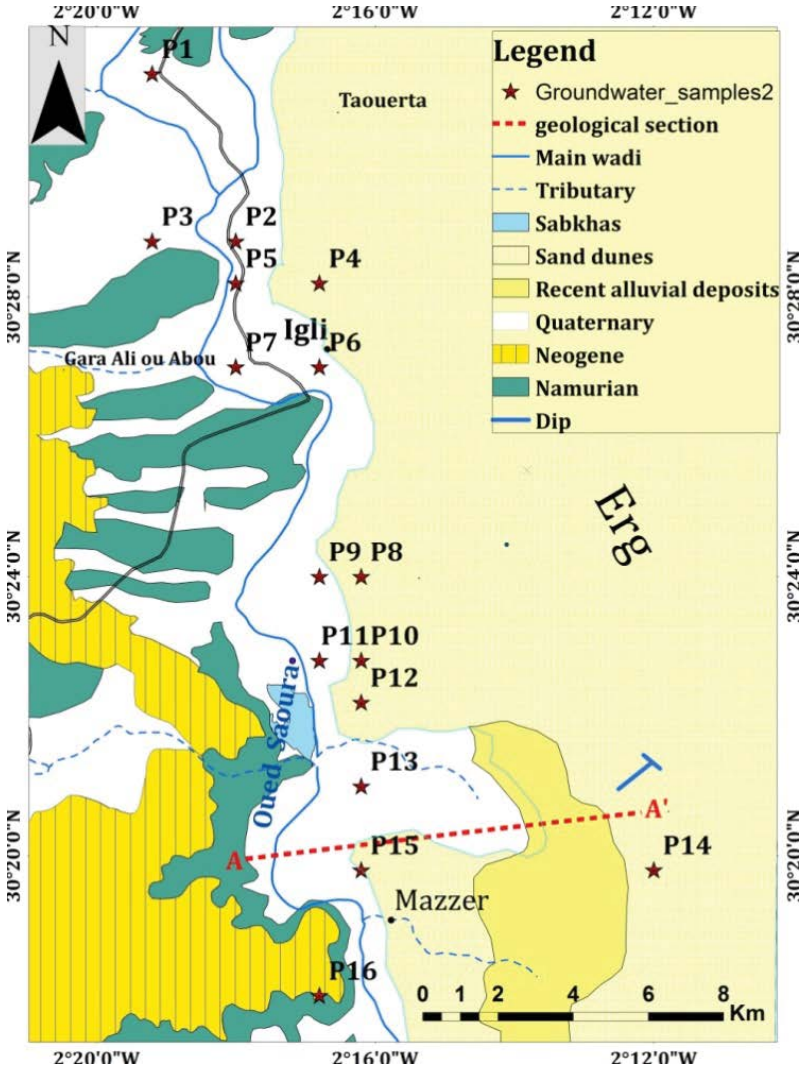

Fig. 2. Geological map of the study area (Extract from the Béni Abbès geological map1/200,000) (Royal Museum for Central Africa, 2014).

and were considered unsafe for drinking water. The values of TDS follow an identical pattern to that of the EC, and they vary from 329 to 8,866 mg/L, with an average of 4,652.68 mg/L, reporting that more than 93.75% of the samples are above the permissible threshold of 1,000 mg/L.

Based on the TDS categorization of groundwater [7], only one sample has an acceptable quality for consumption, while the largest number of other samples have a salty taste with TDS > 1,000 mg/L. This results from groundwater processes, such as aquifer lithology, and climatic and anthropogenic factors [37]. The maximum EC and TDS values occurred in the northern half of the study area, near the Wadi Saoura. They are probably due to the impact of salt enrichment due to water-rock contact [38]. The concentration of total hardness (TH) varies from 16 to 396°F (Fig. 4). This result indicates that the majority of water points (87.5%) in the study area are of very poor quality (TH > 54°F), and this could be related to the high levels of Ca^{2+} and Mg^{2+} resulting from the dissolution of the limestone layers [39].

3.2. Chemical parameters

Individual anion concentrations range from Cl^- (40–2,500 mg/L); SO_4^{2-} (40–3,500 mg/L); HCO_3^- (37–366 mg/L); NO_3^- (6.16–123.2 mg/L). The major comparative anion richness order, expressed as percent meq/L, was $SO_4^{2-} > Cl^- > HCO_3^- > NO_3^-$. Bicarbonate concentrations in this area range from 37 to 366 mg/L; only one sample (P11) records a value above the standard (150–350 mg/L) [7]. The dissolution of carbonate rocks and minerals could explain the existence of bicarbonate and the quaternary limestone crust developed in the bed of Oued Saoura [40]. It may also be due to the oxidation of organic matter in the soil layers on the emerged land [41]. Chloride levels in the study area indicate that more than 93.75% of the samples are above the WHO's normal value of 250 mg/L.

Very high chloride concentrations were observed in the northern and middle plains of the study area, along the Oued Saoura. This result can be justified by the direction

Table 1
Results of physical and chemical analyzes of groundwater (2018 sampling campaign)

Nom	pH	Apparent TDS	EC (μS/cm)	TH (mg/L)	Ca^{2+} (mg/L)	Mg^{2+} (mg/L)	Na^{+} (mg/L)	K^{+} (mg/L)	Cl^{-} (mg/L)	SO_4^{2-} (mg/L)	HCO_3^{-} (mg/L)	NO_3^{-} (mg/L)
P1	7.58	7,737.00	12,920.00	3,270.00	652.00	410.00	1,200.00	270.00	1,850.00	3,100.00	244.00	11.43
P2	7.39	8,389.00	14,990.00	3,780.00	700.00	507.50	1,400.00	54.00	2,500.00	3,000.00	213.50	13.51
P3	7.44	7,659.00	12,270.00	3,960.00	656.00	580.00	950.00	118.00	1,450.00	3,500.00	366.00	39.00
P4	7.50	2,605.00	4,080.00	940.00	176.00	125.00	500.00	16.00	750.00	750.00	244.00	43.41
P5	7.44	5,797.00	9,230.00	2,510.00	496.00	317.50	950.00	34.00	1,450.00	2,300.00	213.50	35.67
P6	7.55	5,229.00	8,340.00	2,400.00	400.00	350.00	796.00	23.40	1,250.00	2,100.00	213.50	95.23
P7	7.21	4,458.00	7,330.00	1,470.00	168.00	263.00	875.00	225.00	1,400.00	1,400.00	116.00	11.00
P8	7.97	5,586.00	8,960.00	2,100.00	400.00	275.00	1,100.00	72.00	1,700.00	1,800.00	213.50	25.88
P9	7.39	8,866.00	14,380.00	3,630.00	820.00	395.00	1,600.00	9.70	2,500.00	3,200.00	335.50	6.16
P10	7.02	1,096.00	1,660.00	420.00	80.00	55.00	180.00	8.10	270.00	280.00	152.50	70.00
P11	7.87	5,312.00	8,870.00	1,840.00	320.00	260.00	1,100.00	22.00	1,700.00	1,700.00	183.00	26.95
P12	7.84	1,949.00	3,030.00	650.00	156.00	65.00	400.00	15.00	600.00	500.00	152.50	60.00
P13	7.50	329.00	547.00	160.00	46.00	11.00	34.00	2.20	40.00	40.00	125.00	31.00
P14	8.83	1,577.00	2,710.00	650.00	124.00	85.00	300.00	23.60	480.90	318.24	122.00	123.20
P15	7.78	1,999.00	3,140.00	940.00	257.00	74.00	260.00	10.70	395.00	925.00	37.00	40.00
P16	7.13	5,855.00	9,240.00	2,810.00	772.00	220.00	820.00	8.30	1,280.00	2,500.00	213.50	41.33

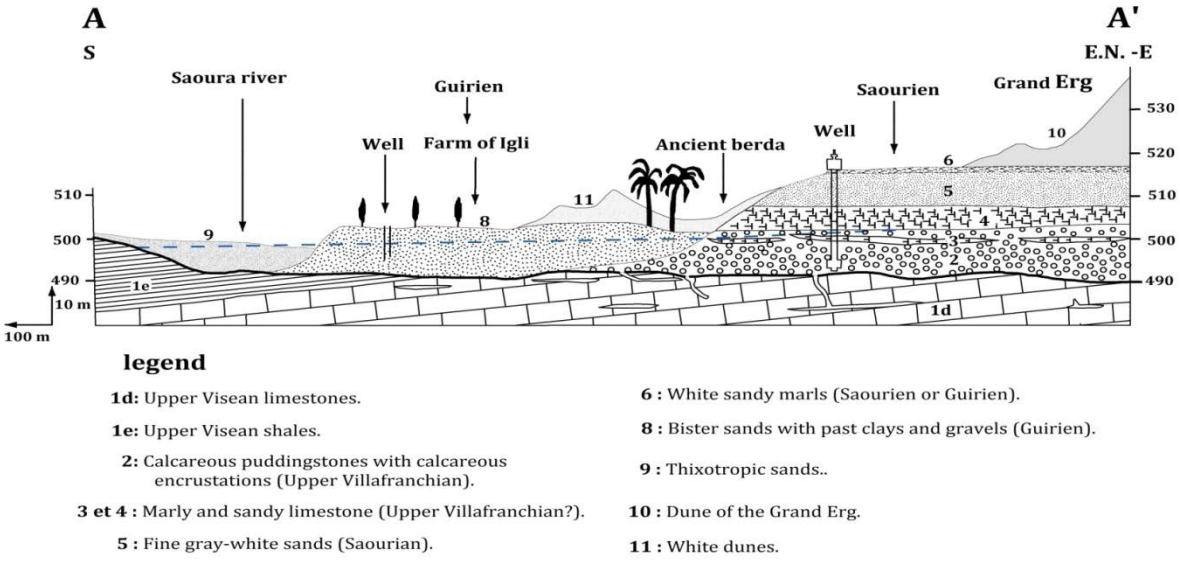

Fig. 3. Geological section of the study area [31].

of groundwater flow, residence time, and reactions in the system in the form of salt accumulation. The high chloride content of the groundwater is probably also due to the infiltration of excess moderately mineralized irrigation water (Fig. 5) [42,43]. The highest values of sulfate concentration in groundwater show that more than 93.75% of the samples exceed the WHO standard (200 mg/L). They could result from the dissolution of gypsum outcrops in the research area [44,45] (Fig. 6).

The nitrate levels in the study area (Fig. 6) reveal that most parts of the area have values between 6.16 and 50 mg/L, with an average value equal to 42.11 mg/L. Only 4 samples were recorded with nitrate concentrations above the 50 mg/L thresholds established by the World Health Organization standards [7]. These may be related to excessive fertilizer use in agricultural plots and palm groves along the stream that runs through the research area [46,47]. The highest nitrate readings are noted in the middle part of the study area, especially in irrigated areas located in the ancient Quaternary formations represented by conglomerate and pebbles, limestone crust, and alluvial fan. The concentration of main cations in the groundwater samples would range from Ca^{2+} (46–820 mg/L); Mg^{2+} (11–580 mg/L); Na^{+} (34–1,600 mg/L) and K^{+} (2.2–270 mg/L). The order of relative

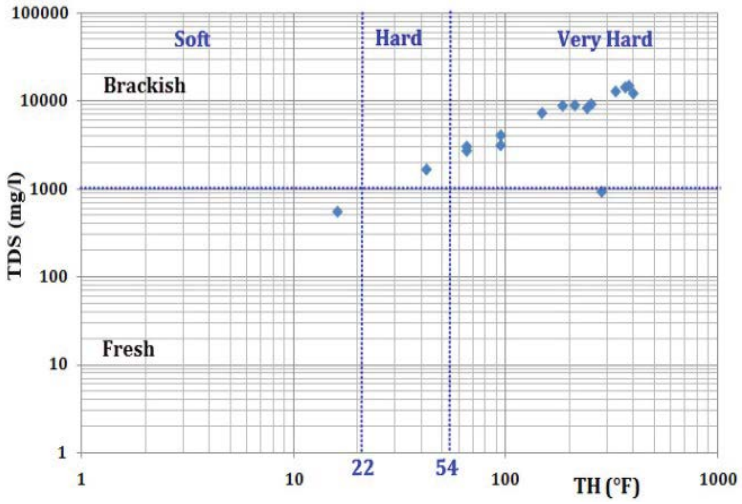

Fig. 4. Graph of apparent TDS (mg/L) vs. TH (°F).

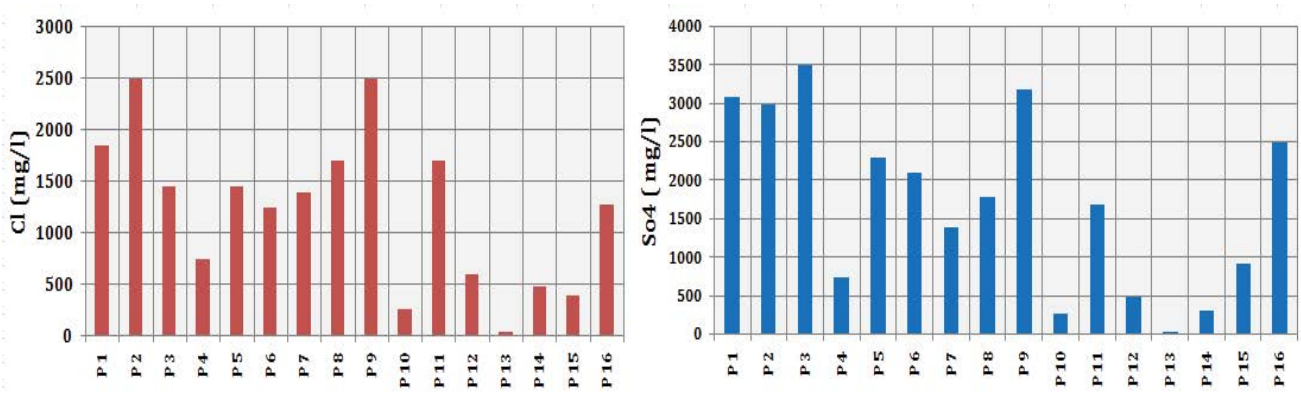

Fig. 5. Bar graph of chloride ion Cl^- and sulfate ion SO_4^{2-} (mg/L) concentrations in the groundwater of the study area.

abundance of major cations, expressed as percent meq/L, was $Ca^{2+} > Na^+ > Mg^{2+} > K^+$.

According to the World Health Organization (WHO) guide, the recommended daily calcium intake for an adult (19–50 y) is 1,000 ppm [48]. As for drinking water, the calcium concentration should not exceed 200 mg/L [7]. The majority of wells in this area have significant amounts of Ca^{2+} concentration (more than 60%) in accordance with the WHO recommendations (Fig. 6). This is due to the lithological deposits of the subsoil and the dissolution of compacted detrital sedimentary rocks [49]. Very high calcium levels in drinking water have harmful and dangerous consequences for human health. They stimulate vascular degeneration (arteriosclerosis) and osteogenesis (osteoarthritis) and can interfere with the absorption of extravital mineral components by the human body [50].

High magnesium levels can cause an undesirable taste in drinking water and significantly alter digestive patterns (Diarrhea) when magnesium is associated with high sulfate concentrations above 700 mg/L [51]. More than 60% of the samples exceed the WHO guidelines (200 mg/L) for sodium (Na^+) in the study area. This result can be related to silicate weathering or cation exchange [52] or anthropogenic actions such as the presence of organic contamination. (Untreated sewage discharge) accompanied by the discharge of fertilizers used in agriculture [53]. High sodium levels in drinking water can be a significant problem for consumers with kidney problems, high blood pressure, or heart disease [54].

Generally, groundwater has potassium concentrations above 10 mg/L. Potassium levels result from weathering of silicate formations (gneisses and shales), potassium clay, and leaching of chemical fertilizers into groundwater (intense fertilization applied in agricultural practices); it can also come from residential and manufacturing waste [55]. In the study area, more than 62.5% of the samples in this area exceed the maximum allowable limit of potassium in drinking water at 12 mg/L [56].

The correlation matrix analyzes correlations between groundwater chemical characteristics and conveys pollution data for better water quality management [57] (Table 2). Strong positive correlations were noticed between apparent TDS and EC, Ca^{2+}, Mg^{2+}, Na^+ and Cl^-, SO_4^{2-} and HCO_3^-, and EC and Ca^{2+}, Mg^{2+}, Na^+ and Cl^-, SO_4^{2-} and HCO_3^-. The strong positive correlation between Na^+, Mg^{2+}, and Cl^- confirms that

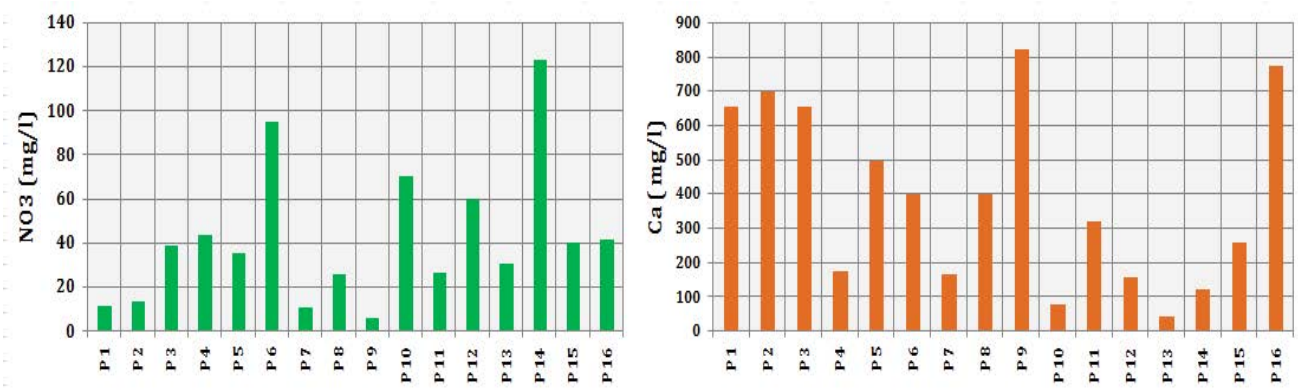

Fig. 6. Bar graph of nitrate NO_3^- and calcium Ca^{2+} (mg/L) concentrations in groundwater in the study area.

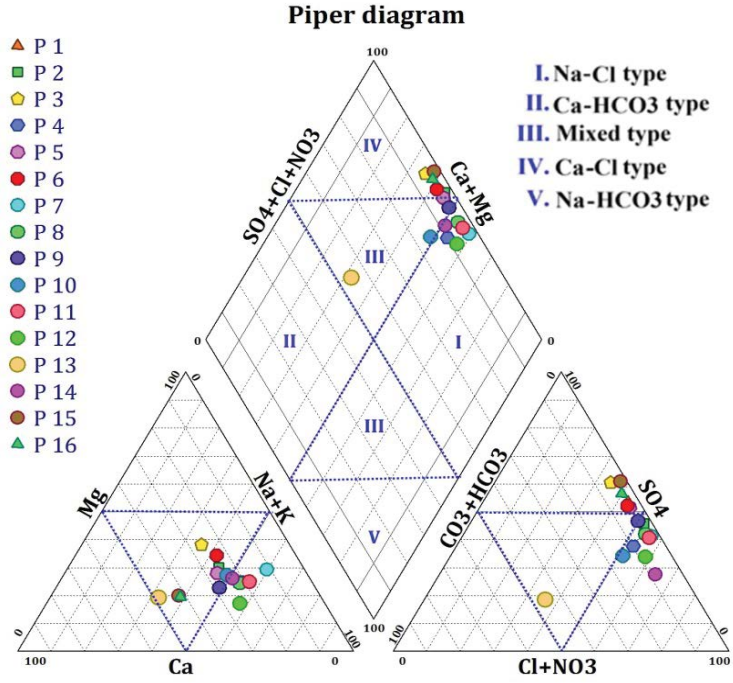

Fig. 7. Piper diagram illustrating the hydrochemical facies of groundwater samples in the study area.

there is a mixing of groundwater samples with saltwater, affirming the impact of lithologic formations on the concentration of these parameters in groundwater; There is also a strong positive correlation between Ca^{2+}, Mg^{2+}, Na^+ and Cl^-, SO_4^{2-} and HCO_3^-. These are inherent indicators of the importance of these parameters in the groundwater chemistry of the study area [58]. Moderate positive correlations were identified between Na^+ and Cl^- and HCO_3^-, suggesting that these parameters also significantly impact the groundwater chemistry of this aquifer.

The low correlation of K^+ with the other ions can be justified by the different origin of this ion with the other chemical parameters. K^+ can be derived from the weathering of feldspar and clay. NO_3^- can result from fertilizers and manure used in agriculture. pH values correlate poorly with other groundwater parameters and do not follow any consistent trend.

3.3. Hydrochemical facies

The groundwater chemistry of the study area was evaluated by arranging the samples on the Piper trilinear diagram [59]. The use of groundwater as a solution to the problem of cationic components was advocated (Ca^{2+}, Mg^{2+} and alkali metals), anionic components (SO_4^{2-}, Cl^-), and components that affect the degree of alkalinity (carbonate (CO_3^{2-}) and HCO_3^-). Groundwater types were defined by a combination of cation and anion domains.

The pyramid feature shows that most of the samples are clustered at the junction of Zone I and IV in equal

Table 2
Correlation matrix of hydrochemical parameters

Variables	pH	Apparent TDS	EC	Ca^{2+}	Mg^{2+}	Na^{+}	K^{+}	Cl^{-}	SO_4^{2-}	HCO_3^{-}	NO_3^{-}
pH	1										
Apparent TDS	–0.2630	1									
EC	–0.2502	0.9969	1								
Ca^{2+}	–0.3004	0.9205	0.9098	1							
Mg^{2+}	–0.2435	0.9362	0.9373	0.8065	1						
Na^{+}	–0.1865	0.9574	0.9595	0.8208	0.8464	1					
K^{+}	–0.1296	0.3959	0.4016	0.1966	0.4565	0.3620	1				
Cl^{-}	–0.1908	0.9521	0.9612	0.8153	0.8493	0.9946	0.3482	1			
SO_4^{2-}	–0.3114	0.9765	0.9663	0.9446	0.9433	0.8759	0.3943	0.8657	1		
HCO_3^{-}	–0.2720	0.7430	0.7170	0.7107	0.7491	0.6618	0.1526	0.6296	0.7566	1	
NO_3^{-}	0.5147	–0.5357	–0.5420	–0.4498	–0.4133	–0.5824	–0.4073	–0.5781	–0.4886	–0.2843	1

proportion (37.5%), indicating that there is a mixture of alkaline earth metals (Ca^{2+}) and alkali (Na^{+}). Concerning cations and anions, most samples indicate the respective dominance of Ca^{2+} and Cl^{-}. Three hydrochemical facies in this aquifer can be recognized on the diagram (Fig. 7). The Ca^{2+}–Cl^{-} water type is the first dominant facies comprising 6 samples. This facies is related primarily to the geological origin (alluvial formations) and secondarily to the result of evaporation in the aquifer (an arid region with shallow groundwater depths <20 m) and may be caused by the dissolution of carbonate rocks in sandstone units, limestones and clay minerals in alluvial deposits [60].

Six samples belong to the Na^{+}–Cl^{-} water type, estimated as the second dominant water type. Silicate weathering, the main hydrochemical process of this facies, relies on ion exchange and mixing fresh groundwater with saline groundwater. Four samples (25%) belong to the mixed facies Cl^{-}–Ca^{2+}–Mg^{2+}, This type of water is formed by the combination of several parameters: geological origin (water-rock ion exchange), evaporation, and the direction of flow (accumulation of mineral salts) and anthropogenic effects [61]. For the last water point, we observe a sample (P13) that appears far from the rest of the points and approaches the facies of Ca–HCO_3. This sample has low TDS levels, indicating the dilution process following rainwater infiltration and illustrates the impact of rainwater recharge [62].

3.4. Analysis of the main components

Eleven variables Ca^{2+}, Mg^{2+}, Na^{+}, K^{+}, Cl^{-}, SO_4^{2-}, HCO_3^{-}, NO_3^{-}, pH, EC, and apparent TDS were analyzed to determine the principal components of the 16 samples collected from the study area. An orthogonal Varimax rotation with Kaiser–Meyer normalization was used to identify the principal components in XLSTAT.

The bi-plot projection shows that three components (factors) have Eigenvalues >1 and are the extracted principal components, as shown in Table 3. The two principal components (factors) explain 80.93% of the total variance in the data (Fig. 8). The factor loading is classified as strong, moderate, and weak, corresponding to absolute loading values of >0.75, 0.75–0.50, and 0.50–0.30, respectively [63]. Component 1, with the highest variance of 70.65% for the combined dataset, reflects the highly mineralized character of the groundwater. High positive loadings >0.56 reveal that the chemical structure factors are mainly Ca^{2+}, Mg^{2+}, Na^{+}, Cl^{-}, SO_4^{2-}, and HCO_3^{-}. They have high loads, which are assumed to be related to geo-climatic conditions, multifaceted natural processes, and anthropogenic toxic wastes. Component 2 explains 10.28% of the total variance, with a strong positive loading between pH and NO_3^{-}. pH may be related to variations in groundwater mineral configuration and mixing of rainwater and groundwater through deep infiltration. Levels of HCO_3^{-} values in groundwater can result from minerals dissolution in saturated and unsaturated zones [64].

3.5. Control mechanisms of groundwater chemistry

3.5.1. Evaporation and alteration of silicates

Groundwater quality is influenced by various variables, including storm water infiltration, aquifer geological formation, mineral content, mineral dissolution, precipitation, seawater intrusion, and anthropogenic impacts [65]. The Gibbs graph [66] can be used to categorize the three main hydro geochemical processes governing groundwater chemistry in an aquifer, namely evaporation/crystallization and water-rock interactions [67]. A significant level of Ca^{2+} and HCO_3^{-} denotes rock-water interaction, and a high level of Na^{+} and Cl^{-} exposes evaporation/crystallization processes. The Gibbs diagram was used to report the chemical data of the groundwater samples (Fig. 9). Only one sample shows a chemical change in the rock-forming minerals and influences groundwater quality by dissolving the rocks through which the water flows, suggesting a chemical change in the rock-forming minerals. The rest of the samples represent evaporation dominance, and most of the samples that fall into evaporation dominance were collected from boreholes drilled near the river. Evaporation causes an increase in salinity by also increasing Na^{+} and Cl^{-} relative to the increase in apparent TDS. In addition, anthropogenic activities and irrigation practices (agricultural fertilizers) also affect evaporation by increasing Na^{+} and Cl^{-}, and therefore apparent TDS [68].

The evaporation process is not only a regular phenomenon in surface water but also groundwater. The Na^+/Cl^- vs. EC graph was used to describe the influence of evaporation on groundwater chemistry. This graph would provide a horizontal line, indicating halite concentration by evaporation, evapotranspiration, and dissolution. Normally, the Na^+/Cl^- ratio is nearly equal to that attributed to halite dissolution, while a ratio greater than (1) generally indicates the release of Na^+ due to silicate deterioration [6]. In the study area, it can be seen that Na^+/Cl^- ratios decrease with increasing EC. The Na^+/Cl^- molar ratio for groundwater samples from the Igli infero-flow ranges from 0.98 to 1.30 (Fig. 10). Most samples have a Na^+/Cl^- molar ratio greater than "1", which is generally interpreted to be due to sodium release from a silicate weathering reaction. However, water points with a Na^+/Cl^- molar ratio of less than "1" indicate halite dissolution was the primary process. EC vs. Na^+/Cl^- scatter plot shows a sloping trend line, indicating that evaporation may not be the primary geochemical process controlling groundwater chemistry [69].

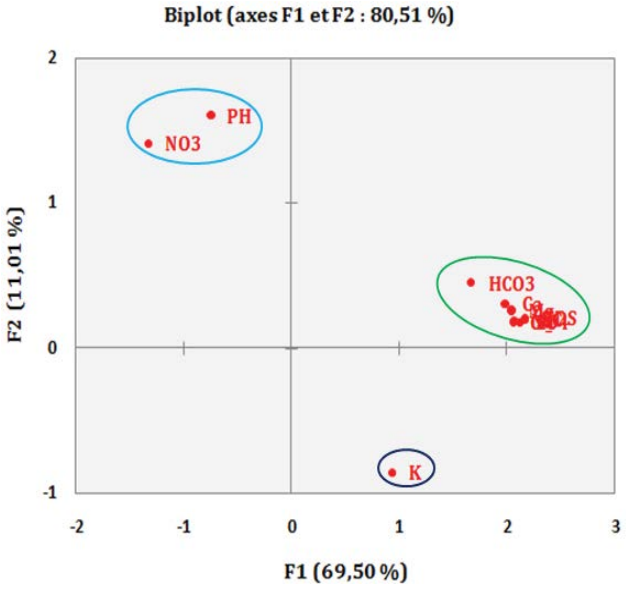

Fig. 8. Projection of variables onto the factorial plane (1 × 2) of the Igli alluvial aquifer.

Table 3
Principal component matrices with Varimax rotation and groundwater sample variables

Variables	F1	F2
pH	0.1113	**0.5141**
TDS	**0.8228**	0.0082
EC	**0.9837**	0,0042
TH	**0.9466**	0.0135
Ca^{2+}	**0.8080**	0.0135
Mg^{2+}	**0.8935**	0.0108
Na^+	**0.8916**	0.0032
K^+	0.1733	0.1818
Cl^-	**0.8820**	0.0030
SO_4^{2-}	**0.9482**	0.0035
HCO_3^-	**0.6641**	0.0493
NO_3^-	0.3527	**0.4284**
Eigenvalues	8.4779	1.2335
Initial Eigenvalues of variances in %	70.6489	10.2792
Cumulative % of variance	70.6489	80.9281

Na⁺ and Cl⁻ are important natural ions, and if the sodium in groundwater were from halite alteration [70], the concentrations of sodium and chloride would be very close to the 1:1 line in the Na^+ vs. Cl^- [71]. Most groundwater samples do not lie along with the 1:1 line in the present work. Therefore, it is clear from the graph (Fig. 11) that the chemistry of sodium and chloride in the region cannot be explained solely based on halite dissolution processes because halite dissolution releases nearly equal amounts of sodium and chloride into the solution. In the present study, it is observed that the Na^+/Cl^- ratio in water is greater than 1 in almost all samples. This may explain that the main supplier of Na^+ is silicate weathering and therefore suggests that a higher sodium concentration may be added due to rock weathering or human activities compared to atmospheric precipitation [6].

To verify the carbonate weathering process, the scatter plot of $(Ca^{2+} + Mg^{2+})$ and $(Na^+ + K^+)$ against the total cation plot was used [72]. Fig. 12 shows that all the plotted points are less than 1:1 equiline with an equivalent ratio on average of 0.53 ± 0.07 for $Ca^{2+} + Mg^{2+}/\sum$cations. While the ratios of $(Ca^{2+} + Mg^{2+})/(Na^+ + K^+)$ were 1.19 ± 0.33, in contrast, the $Na^+ + K^+/\sum$cations ratios were low at 0.47 ± 0.07. The high levels of $Ca^{2+} + Mg^{2+}/\sum$cations and $(Ca^{2+} + Mg^{2+})/(Na^+ + K^+)$ ratios and the low $Na^+ + K^+/\sum$cations ratios indicate that carbonate alteration is the dominant mechanism controlling the major ion chemistry of the Igli alluvial aquifer, with a minor contribution from silicate alteration.

3.5.2. Ion exchange process

The $(Ca^{2+} + Mg^{2+})$ vs. HCO_3 diagram was applied to better understand the mechanism that influences groundwater calcium concentrations [68,73] (Fig. 13). The low molar ratios (<0.5) of $Ca^{2+} + Mg^{2+}/HCO_3^-$ can be explained by the exchange of calcium and magnesium in the water or by the enrichment of HCO_3^- possibly due to weathering with silicates [74]. In contrast, high ratios (>0.5) suggest other sources of Ca^{2+} and Mg^{2+}, for example, reverse ion exchange that can be detected in hard rock layers and increased salinity [75]. In the study area, the $Ca^{2+} + Mg^{2+}$ molar ratio ranges from 1.60 to 40.24 and may be caused by the dissolution of the Quaternary limestone crust (reverse ion exchange). Most samples are below the 1:1 line, demonstrating that silicate alteration is dominant and contributes to HCO_3^- to the groundwater [76]. Ion exchange is one of the major mechanisms contributing to groundwater ion concentrations. The chlor-alkali indices 1 and 2 (CAI-1 and CAI-2), calculated for groundwater samples in the basin, clearly imply ion-exchange activity.

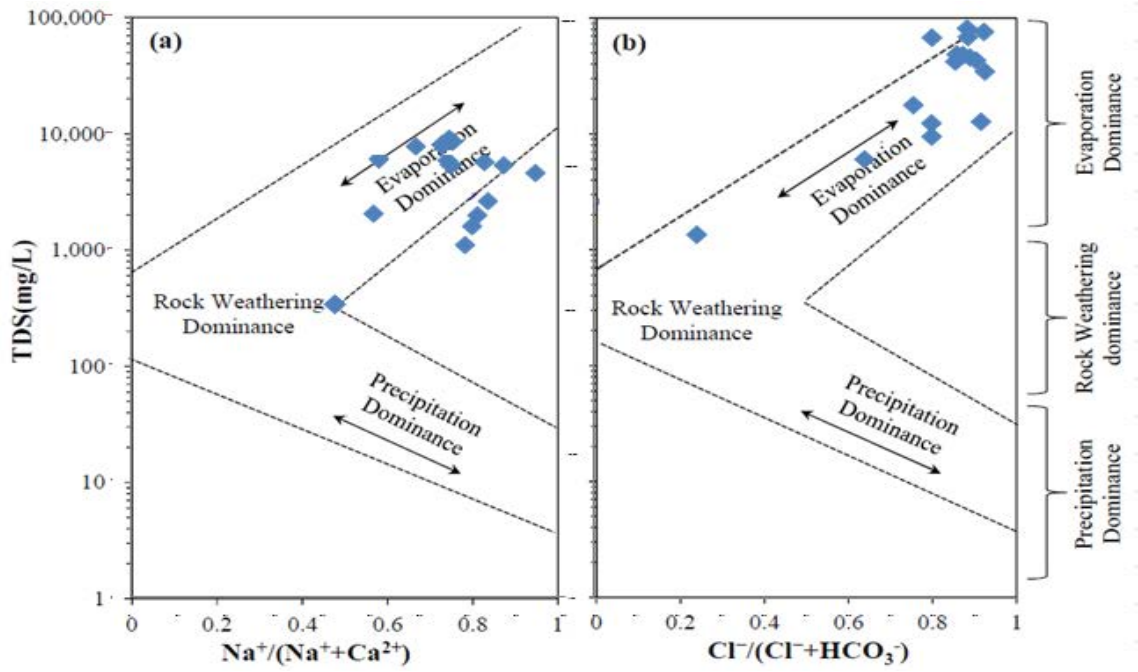

Fig. 9. Gibbs diagram.

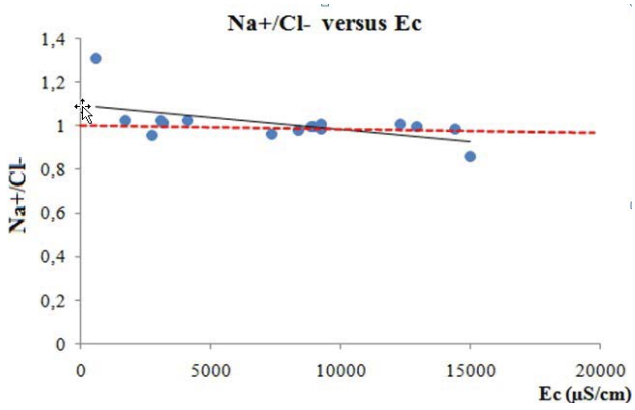

Fig. 10. Diagram of Na^+/Cl^- as a function of EC.

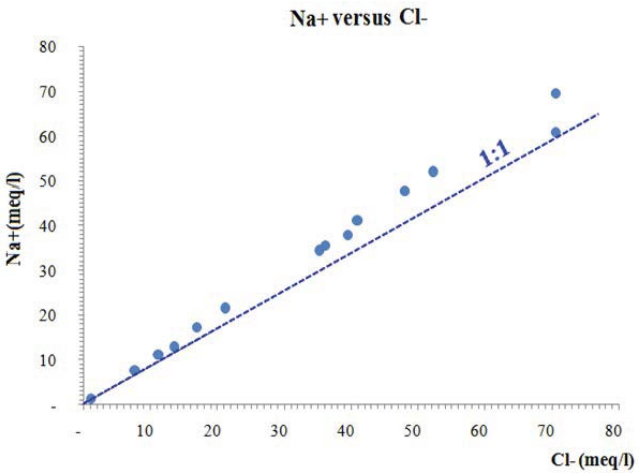

Fig. 11. Diagram of Na^{+-} as a function of Cl^-.

$$\text{CAI 1}: \frac{\left(r\text{Cl}^- - \left(r\text{Na}^+ + rK^+\right)\right)}{r\text{Cl}^-} \quad (1)$$

$$\text{CAI 2}: \frac{\left(r\text{Cl}^- - \left(r\text{Na}^+ + rK^+\right)\right)}{\left(r\text{SO}_4^{2-} + r\text{HCO}_3^- + r\text{NO}_3^-\right)} \quad (2)$$

where the units of the chemical parameters are in meq/L.

When exchange takes place between Ca^{2+} or Mg^{2+} in the groundwater with Na^+ and K^+ in the aquifer, both of the above indices are negative; a reverse ion exchange then means that both indices will be positive [77]. From (Fig. 14), it can be seen that the majority of the CAI values for the groundwater samples in CAI-1 and CAI-2 were negative. Therefore, the exchange of Ca^{2+} + Mg^{2+} with Na^+ and K^+ is the predominant cation exchange process, while three samples (P1, P3, and P5) remained positive. This indicates that reverse cation exchange occurred at these locations.

3.5.3. Saturation index

The thermodynamic process can be determined via the calculation of mineral equilibrium. In a groundwater system, SI can help recognize the presence of certain dominant thermodynamic processes [78]. SI values for relevant minerals were determined using the PHREEQC program. If the SI is zero, it expresses solubility equilibrium as a function of the mineral composition of the water. An SI less than zero indicates that the groundwater

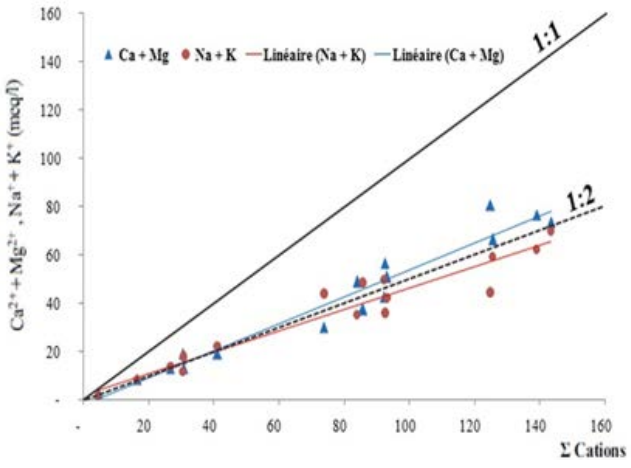

Fig. 12. Point cloud of $Ca^{2+} + Mg^{2+}$ and $Na^{+} + K^{+}$ vs. total cations.

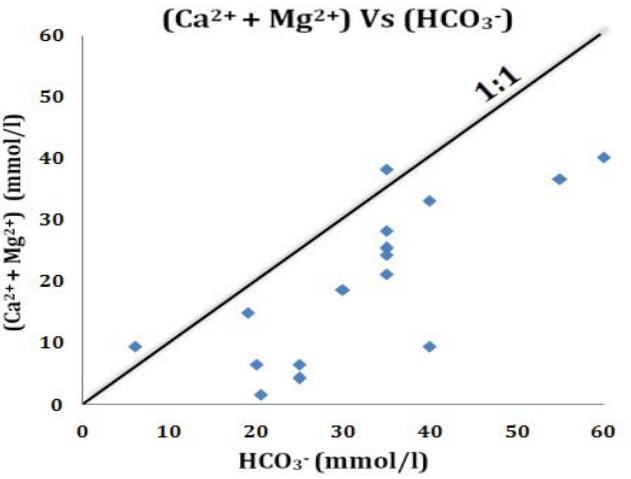

Fig. 13. Point cloud of $Ca^{2+} + Mg^{2+}$ vs. HCO_3.

is under saturated with respect to that mineral, and if it is greater than 0, it shows that the groundwater is supersaturated with that specific mineral and therefore cannot dissolve many minerals. As shown in Table 4, equilibrium is assumed to be between SI = –0.1 and 0.1 [79]. SI values for aragonite, calcite, and dolomite range from –0.65 to 1.08, –0.51 to 1.22, and –0.84 to 2.63, respectively, with an average of 0.29, 0.43, and 0.98. Most samples are saturated with these minerals (Fig. 15). The SI values for anhydrite, halite, and gypsum range from –2.34 to –0.15, –7.13 to –4.16, and –2.12 to 0.07, respectively, suggesting that the samples are not saturated with anhydrite, gypsum, and halite (Fig. 15). This means that the samples tend to dissolve these minerals continuously due to the impact of precipitation and irrigation water before reaching the groundwater [80].

3.6. Assessment of water resources for irrigation

Agriculture is crucial for meeting the population's food needs in many nations worldwide, especially in Third World countries experiencing a large population explosion. On the other hand, agricultural activities have a well-established impact on groundwater quality, but there is very little information on how these activities ultimately influence groundwater quality. Many hydro-geochemical reactions can occur, and the mixing of these activities determines the composition of groundwater. The degradation of groundwater quality in these countries is a major obstacle to its use in agriculture. Recognizing that the suitability of groundwater for irrigation depends on its mineral constituents, many studies have been conducted to assess its suitability [81–83]. Many studies have assessed its suitability. In this study, the groundwater produced by the alluvial aquifer is mainly used for irrigation in the Igli area. Thus, it becomes essential to evaluate the quality and suitability of groundwater for irrigation. Parameters such as EC, sodium adsorption rate (SAR) [Eq. (3)], percent sodium (Na%) [Eq. (4)], and magnesium hazard (MH) [Eq. (5)] were employed to estimate the suitability of the studied groundwater for irrigation purposes. Table 5 summarizes the results of the calculated values.

According to Table 1, the EC values range from 547 to 14,990 μS/cm with a mean value equal to 7,606.06 μS/cm. This wide variation in EC conductivity values is mainly attributed to the lithological composition and anthropogenic activities prevalent in this region. In general, irrigation water with an EC value <700 μS/cm does not threaten most crops, while its value >3,000 μS/cm can limit their growth [84]. Based on the classification of [85] (Fig. 16), the studied water samples are classified into 4 categories. A medium salinity risk is represented by only one sample (P18), the last one with a high risk (P23), and a very high salinity risk (4 samples), providing a respective distribution of 6.25%, 6.25%, and 25. While the rest of the samples, 10 in number, provided salinity values outside the values of the form and are considered unsuitable for irrigation. Water with a high salinity hazard rating (C3) can harm sensitive crops and other plants. Careful management practices should be used in such a circumstance. Water with very high salinity (C4) is not suitable for ordinary irrigation practices but can be useful for plants with high salt tolerance and through specific soil preparation practices

3.7. Alkaline danger

While high amounts of salt (high EC) in water cause the development of saline soils, high levels of sodium (SAR) cause the development of alkaline soils [86]. Irrigation with Na^{+} enriched water results in ion-exchange reactions, that is, absorption of Na^{+} and release of Ca^{2+} and Mg^{2+}. This type of reaction causes the soil aggregates to disperse, reducing their permeability [87]. The presence of sodium or alkaline risk in the irrigation water is measured by the total and relative concentration of cations expressed as SAR. The following formula is used to calculate SAR, where all ionic concentrations are expressed in meq/L [19]:

$$\left(\mathrm{SAR}\right) = \frac{\mathrm{Na}^{+}}{\sqrt{\mathrm{Ca}^{2+} + \mathrm{Mg}^{2+}/2}} \tag{3}$$

Table 4
Saturation index (SI) of relevant minerals

Sample	Anhydrite	Aragonite	Calcite	CO_2 (g)	Halite	Dolomite	Gypsum
P1	–0.23	0.61	0.76	–2.33	–4.4	1.65	–0.01
P2	–0.24	0.4	0.54	–2.21	–4.21	1.29	–0.02
P3	–0.2	0.64	0.78	–2.02	–4.61	1.85	0.01
P4	–1.01	0.22	0.36	–2.19	–5.1	0.91	–0.79
P5	–0.38	0.36	0.5	–2.23	–4.59	1.16	–0.16
P6	–0.48	0.4	0.54	–2.34	–4.72	1.36	–0.27
P7	–0.94	–0.52	–0.37	–2.24	–4.62	–0.21	–0.72
P8	–0.54	0.81	0.95	–2.78	–4.45	2.08	–0.32
P9	–0.15	0.65	0.79	–2.01	–4.16	1.61	0.07
P10	–1.53	–0.65	–0.51	–1.88	–5.93	–0.84	–1.31
P11	–0.63	0.56	0.71	–2.73	–4.45	1.67	–0.42
P12	–1.14	0.35	0.5	–2.73	–5.27	0.96	–0.92
P13	–2.34	–0.33	–0.19	–2.41	–7.43	–0.65	–2.12
P14	–1.39	1.08	1.22	–3.91	–5.48	2.63	–1.17
P15	–0.73	–0.16	–0.02	–3.29	–5.65	–0.24	–0.51
P16	–0.16	0.24	0.38	–1.92	–4.71	0.55	0.05
Max.	–0.1500	1.08	1.2200	–1.8800	–4.1600	2.6300	0.0700
Min.	–2.3400	–0.65	–0.5100	–3.9100	–7.4300	–0.8400	–2.1200
Mean	–0.7556	0.2913	0.4338	–2.4513	–4.9863	0.9863	–0.5381
SD	0.6116	0.4823	0.4820	0.5375	0.8336	1.0115	0.6099

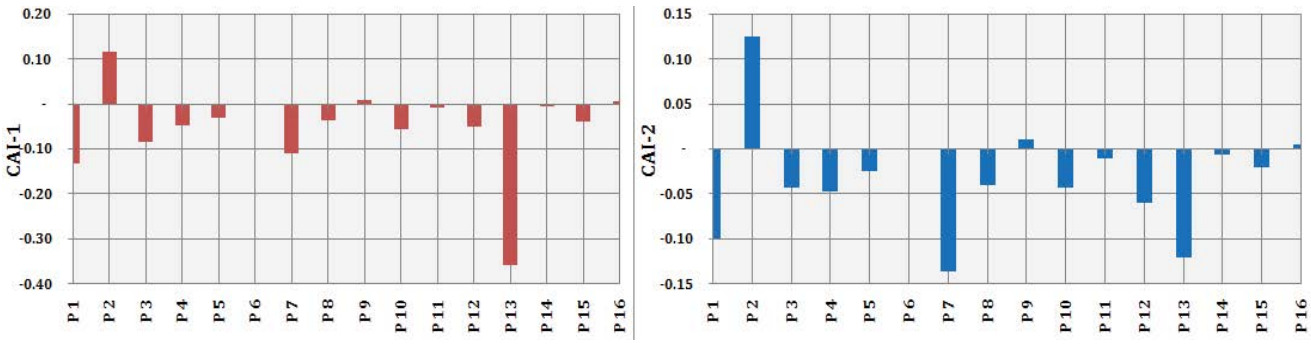

Fig. 14. Bar graph of the chloro-alkaline indices CAI-1 and CAI-2.

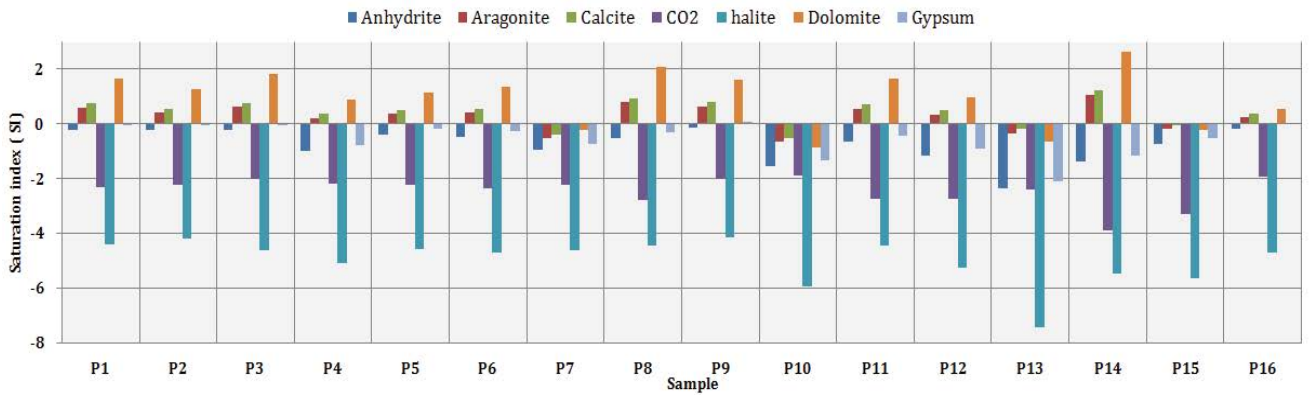

Fig. 15. Variation of the SI saturation index.

The amount of salt absorbed by soils is related to the SAR levels of the irrigation water. Due to the large amounts of salt absorbed colloidally, the continuous use of water with high SAR values degrades the soil's physical structure. This decomposition then causes the clay in the soil to disperse, making it hard and compact when it is too dry and more impervious to water infiltration due to dispersion and expansion when it is wet [88]. The calculated SAR values in the studied samples range from 1.17 to 11.48 (Table 5). The SAR values plotted in the diagram (Fig. 16) are divided into four classes, from low (12.50%), medium (25.50%), high (31.25%) to very high (31.25%). According to Richard's (1954) classification [85] applied to the calculated SAR values, (1) the water sample falls in the good category, (1) in the medium category, (4) as polluted, and (10) classified as unsuitable.

3.8. Sodium content (Na%)

The concentration of sodium in the irrigation water is also represented as the percentage of sodium (percent Na), which can be determined by applying the following equation, where all ionic values are given in meq/L:

$$\left(\mathrm{Na\%}\right)=\frac{\mathrm{Na}^{+}+K^{+}}{Ca^{2+}+\mathrm{Mg}^{2+}+\mathrm{Na}^{+}+K^{+}}\times 100 \tag{4}$$

Na% is classified as excellent (<20%), good (20%–40%), eligible (40%–60%), questionable (60%–80%), and inadequate (>80%) [89]. The values of the percentage of sodium in the studied groundwater samples range from 32.42 to 59.31% (Table 5). It can be noted that (4) samples have good sodium content (20%–40%) and the rest of the samples (62.50%) are in the eligible category.

Table 5
Sodium adsorption ratio, sodium rate, and MH values for the study area

Name	X	Y	SAR	Na%	MH
P1	–2.32	30.52	9.06	47.11	50.86
P2	–2.3	30.48	9.82	44.78	54.41
P3	–2.32	30.48	6.51	35.5	59.27
P4	–2.28	30.47	7.04	53.71	53.9
P5	–2.3	30.47	8.18	45.3	51.31
P6	–2.28	30.45	7.01	41.91	59.02
P7	–2.3	30.45	9.81	59.31	72.05
P8	–2.27	30.4	10.36	53.82	53.08
P9	–2.28	30.4	11.48	48.71	44.23
P10	–2.27	30.38	3.79	48.52	53.11
P11	–2.28	30.38	11.06	56.41	57.22
P12	–2.27	30.37	6.78	57.47	40.68
P13	–2.27	30.35	1.17	32.42	28.35
P14	–2.2	30.33	5.08	50.84	53.03
P15	–2.27	30.33	3.67	37.92	32.15
P16	–2.28	30.3	6.69	38.74	31.93

3.9. Magnesium hazard

Magnesium is an important element in the hydrochemical makeup of water, but excess of this element tends toward soil alkalinity and influences agricultural yield. The MH value must be <50 to certify water as good for irrigation [90].

The MH is calculated as follows:

$$\mathrm{MH}=\frac{\mathrm{Mg}^{2+}}{\mathrm{Ca}^{2+}+\mathrm{Mg}^{2+}}\times 100 \tag{5}$$

The MH values in the study area range from 28.35% to 72.05%. Five water points are below the standard value of 50. This shows that about 31.25% of water samples are suitable for irrigation.

3.10. Cluster analysis

HCA has long been a widely used method for identifying the clustering of chemical variables in groundwater chemistry. This method is typically used to group variables into clusters based on similarities such that each cluster describes a specific action in a groundwater system [91]. The application of the cluster method was made using the XLSTAT software. Fig. 17 reveals the level of aggregation of a parameter in groundwater. The parameters integrated in the same cluster probably have a similar origin. This study used cluster analysis in R mode to group the groundwater parameters, which allowed the reconstruction of the group into 3 main clusters. Cluster 1 includes pH and NO_3^- and reflects the influence of nitrate on water quality. This could come from anthropogenic sources such as runoff sources and agricultural practices. Group 2 includes only potassium K^+, while group 3 includes the rest of the parameters (HCO_3^-, apparent TDS, Na^+, Cl^-, Ca^{2+}, Mg^{2+}, EC, TH, and SO_4^{2-}).

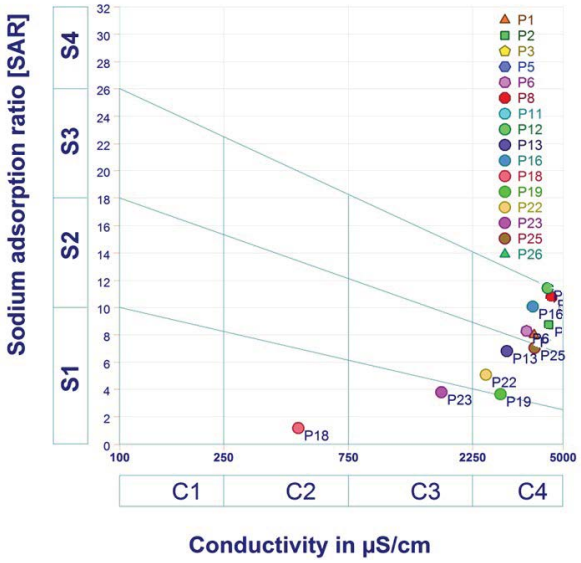

Fig. 16. Water classification based on EC and SAR values.

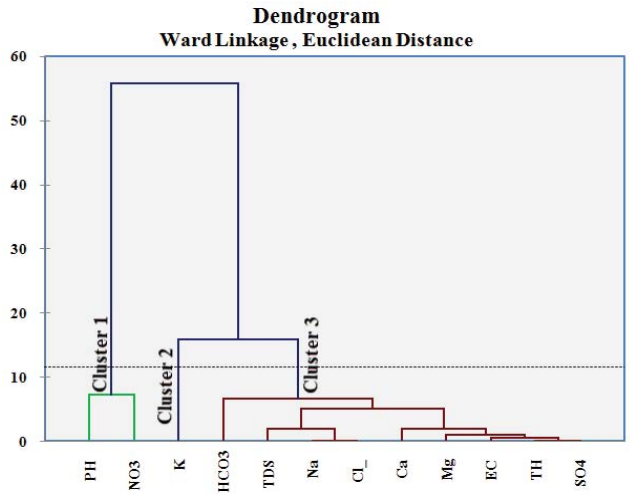

Fig. 17. Dendrogram of observations.

4. Conclusion

This study aimed to conduct a hydrochemical assessment of the infero-flux aquifer in the Igli Region to determine the influence of natural and human variables on the groundwater quality of this region. To achieve this objective, samples were collected from 16 water points in this research region. The studied water points illustrate that slight alkalinity marks the region's groundwater with an average (pH = 7.59) and strong mineralization, defined by high conductivity values. This is due to the presence of ionic interaction between the water and the different geological strata, which leads to the dissolution of minerals. In addition, the excessive and irrational use of water in the region has largely contributed to the acceleration of these reactions. In addition, the human factor in these results may be responsible for the discharge of untreated sewage from the city and septic tanks arbitrarily placed in the research area, and the excessive use of fertilizers and organic matter in the agricultural lands adjacent to the Wadi. However, we cannot be sure because we could not perform a chemical oxygen demand analysis, which is an important indicator of whether there is pollution in the wastewater. Thus, the anionic and cationic classification process revealed that calcium Ca^{2+} and sodium Na^{+} are the dominant cations in groundwater, while chloride Cl^{-} and bicarbonates HCO_3^{-} are abundant anions. This proves that there is a first equilibrium between alkaline earth metals ($Ca^{2+} + Mg^{2+}$) and alkali metals ($Na^{+} + K^{+}$) and a second equilibrium between strong acids ($Cl^{-} + SO_4^{2-}$) and weak acids ($HCO_3^{-} + CO_3^{-}$). Using the Piper diagram, it was concluded that the chemical facies Cl^{-} Na^{+} and Cl^{-} Ca^{2+} are the most dominant, with equal ratios (37.5%) for each facies.

Due to the degradation of carbonate minerals by precipitation and irrigation water, the resulting saturation index (SI) values show that most samples are saturated with the minerals aragonite, calcite, and dolomite. The SI values also show undersaturation for anhydrite, halite, and gypsum due to the dissolution of these minerals. Comparing the values of the studied chemical parameters with the standards described by the World Health Organization reveals that only 45.83% of the studied water points are of good quality and suitable for domestic consumption. In contrast, the remaining water points recorded high concentrations of the apparent parameters TDS, EC, Ca^{2+}, Mg^{2+}, Na^{+}, K^{+}, Cl^{-}, and SO_4^{2-}. According to the study results on the quality of groundwater adaptation for irrigation, more than 79 percent of the water points are acceptable for irrigation. In contrast, the remaining water points are considered unsuitable for irrigation due to the significant potential for adverse effects on soil and wildlife.

Acknowledgements

Special thanks to the anonymous reviewers for many detailed comments and suggestions to improve this work, also we would like to acknowledge the laboratory director of the national agency of hydraulic resources (ANRH-Adrar) and the technician Mrs. Sahraoui Fatiha for their permission to perform all the analyses in the laboratory. We also thank Mrs. Gabriela Kouahla, certified translator – scientific proofreader, for proofreading and linguistic improvement of this manuscript.

References

[1] D.L. Danielopol, G. Christian, G. Amara, J. Notenboom, Present state and future prospects for groundwater ecosystems, Environ. Conserv., 30 (2003) 104–130.
[2] W. Kinzelbach, P. Brunner, A. von Boetticher, L. Kgotlhang, C. Milzow, Sustainable Water Management in Arid and Semi-Arid Regions, In: Water resources of Arid Areas, Taylor & Francis, Oxfordshire, 2004, pp. 3–16.
[3] M. Bazza, K. Melvyn, K. Cody, Drought Characteristics and Management in North Africa and the Near East, FAO Water Reports, Food and Agricultural Organization of the United Nations, 2018. Available at: http://www.fao.org/3/CA0034EN/ca0034en.pdf
[4] K. Sekkoum, M.F. Talhi, A. Cheriti, Y. Bourmita, N. Belboukhari, N. Boulenouar, S. Taleb, Water in Algerian Sahara: Environmental and Health Impact, R.Y. Ning, Ed., Advancing Desalination, IntechOpen, 2012, pp. 197–216.
[5] M. El Kashouty, A.A. Aiman, S. Mamdouh, M. Hany, Hydrogeophysical investigation of groundwater potential in the El Bawiti, Northern Bahariya Oasis, Western Desert, Egypt, Arabian J. Geosci., 5 (2012) 953–970.
[6] M. Meybeck, Global chemical weathering of surficial rocks estimated from river dissolved loads, Am. J. Sci., 287 (1987) 401–428.
[7] WHO, Guidelines for Drinking-Water Quality: Fourth Edition Incorporating the First and Second Edition, World Health Organization, Geneva, 2011.
[8] A. Ambica, Groundwater quality characteristics study by using water quality index in Tambaram Area, Chennai, Tamil Nadu, Middle East J. Sci. Res., 20 (2014) 1396–1401.
[9] M. Nikaeen, A. Shahryari, M. Hajiannejad, H. Saffari, Z.M. Kachuei, A. Hassanzadeh, Assessment of the physicochemical quality of drinking water resources in the Central Part of Iran, J. Environ. Health., 78 (2016) 40–45.
[10] C. Nerbrand, L. Agréus, R.A. Lenner, P. Nyberg, K. Svärdsudd, The influence of calcium and magnesium in drinking water and diet on cardiovascular risk factors in individuals living in hard and soft water areas with differences in cardiovascular mortality, BMC Public Health, 3 (2003) 21, doi: 10.1186/1471-2458-3-21.
[11] C. Munteanu, A. Iliuta, The role of sodium in the body, Balneo PRM Res. J., 2 (2011) 70–74.
[12] N. Graudal, T. Hubeck-Graudal, G. Jürgens, R.S. Taylor, Dose-response relation between dietary sodium and blood pressure:

a meta-regression analysis of 133 randomized controlled trials, Am. J. Clin. Nutr., 109 (2019) 1273–1278.
[13] D.J. Halliwell, K. Barlow, D. Nash, A review of the effects of wastewater sodium on soil physical properties and their implications for irrigation systems, Aust. J. Soil Res., 39 (2001) 1259–1267.
[14] S. Mahato, A. Mahato, P.K. Karna, N. Balmiki, Investigating aquifer contamination and groundwater quality in eastern Terai region of Nepal, BMC Res. Notes, 11 (2018) 321, doi: 10.1186/s13104-018-3445-z
[15] M.H. Ward, R.R. Jones, J.D. Brender, T.M. de Kok, P.J. Weyer, B.T. Nolan, C.M. Villanueva, S.G. van Breda, Drinking water nitrate and human health: an updated review, Int. J. Environ. Res. Public Health, 15 (2018) 1557, doi: 10.3390/ijerph15071557.
[16] R.R. Pant, F. Zhang, F. Ur Rehman, G.X. Wang, M. Ye, C. Zeng, H. Tang, Spatiotemporal variations of hydrogeochemistry and its controlling factors in the Gandaki River Basin, Central Himalaya Nepal, Sci. Total Environ., 622 (2018) 770–782.
[17] Z.J. Yao, R. Wang, Z.F. Liu, S.S. Wu, L.G. Jiang, Spatial-temporal patterns of major ion chemistry and its controlling factors in the Manasarovar Basin, Tibet, J. Geogr. Sci., 25 (2015) 687–700.
[18] L. Yang, X. Song, Y. Zhang, D. Han, B. Zhang, D. Long, Characterizing interactions between surface water and groundwater, Hydrol. Earth Syst. Sci., 16 (2012) 4265–4277.
[19] A. Belkendil, M. Habi, B. Morsli, Evaluation of the physico-chemical quality of groundwater in arid areas: case study (watershed of the Oued Béchar) in Béchar-Kenadsa Region, Desal. Water Treat., 107 (2018) 136–146.
[20] B. Linhoff, P. Longmire, M. Rearick, D. McQuillan, G. Perkins, Water quality and hydrogeochemistry of a basin and range watershed in a semi-arid region of northern New Mexico, Environ. Earth Sci., 75 (2016) 640, doi: 10.1007/s12665-015-5179-8.
[21] Y.X. Chai, C.L. Xiao, M.Q. Li, X.J. Liang, Hydrogeochemical characteristics and groundwater quality evaluation based on multivariate statistical analysis, Water, 12 (2020) 2792, doi: 10.3390/w12102792.
[22] P. Ravikumar, R.K. Somashekar, Assessment and modelling of groundwater quality data and evaluation of their corrosiveness and scaling potential using environmetric methods in Bangalore South Taluk, Karnataka state, India, Water Resour., 39 (2012) 446–473.
[23] S. Odat, Cluster and factor analysis of groundwater in Mafraq Area, Jordan, Curr. World Environ., 10 (2015) 422–431.
[24] H. Baazi, M. Kalla, F.Z. Tebbi, Hydrochemical characterisation of groundwater quality: Merdja Plain (Tebessa Town, Algeria), Civ. Eng. J., 6 (2020) 318–325.
[25] H. Saibi, M. Mesbah, A.S. Moulla, A.H. Guendouz, S. Ehara, Principal component, chemical, bacteriological, and isotopic analyses of Oued-Souf groundwaters (revised), Environ. Earth Sci., 75 (2016) 272, doi: 10.1007/s12665-015-4878-5.
[26] J. Fabre, Introduction a la Géologie du Sahara Algérien et des regions voisines [Introduction to the Geology of the Algerian Sahara and Neighboring Regions], National Publishing and Distribution Company, Algeria, 1976.
[27] AQUASOL, Geophysical Study of the Igli Region, Wilaya of Béchar, National Water Resources Agency (ANRH), Ministry of Water Resources, Unpublished, Algeria, 2009.
[28] A. Mekkaoui, Regional Prospecting for Copper and Silver in the Ugarta Mountains, Final Report, National Office for Geological and Mining Research, ORGM, Unpublished, Algeria, 1998.
[29] C. Pareyn, Les Massifs Carbonifères Du Sahara Sud-Oranais [The Carboniferous Massif of the South Sahara Oranais], Vol. II, Stratigraphic Paleontology, Publications of the Saharan Research Center, Geology Series, CNRS Editions, France, 1961, pp. 1–244.
[30] J. Chavaillon, Étude stratigraphique des formations Quaternaires du Sahara nord-occidental (Colomb- Béchar à Reggane) [Stratigraphic Study of the Quaternary Formations of the North-Western Sahara (Colomb-Béchar in Reggane)], Th. Doc., Publ. CRZA, Géol. Series. 10. CNRS, Paris, 1964, p. 393.
[31] M.A. Roche, Hydrogéologie de la haute Saoura (Sahara Nord Occidental) [Hydrogeology of the Upper Saoura (North Western Sahara)], CNRS (Research on Arid Zones), France, 1973.
[32] N. Yousfi, C. Ait-Ahmed, Contribution à l'étude hydrogéologique de la Grande Source et de la palmeraie de Béni-Abbès (Sahara Occidental) [Contribution to the Hydro-Geological Study of the Grande Source and the Palm Grove of Béni-Abbès (Western Sahara)], Master Thesis, University of Science and Technology of Oran, Algeria, 1992.
[33] H. Mansour, N. Yousfi, Les isotopes dans l'eau du Sahara Nord occidental Algérien (grand erg occidental) [Isotopes in the Water of the Western North Algerian Sahara (Large Western Erg)], 2nd Day of Applied Geology, Sfax, Tunisia, 1993.
[34] T. Merzougui, Caractérisation hydrogéologique et modélisation d'un aquifère alluvial en zone hyper aride: cas de la nappe de la palmeraie de Béni Abbès (vallee de la saoura, sud ouest algérien) [Hydrogeological Characterization and Modeling of an Alluvial Aquifer in a Hyper-Arid Zone: Case of the Béni Abbès Palm Grove Aquifer (Saoura Valley, South-West Algeria)], Master Thesis, University Abou Bekr Belkaid, Algeria, 2011.
[35] A.F. Rusydi, Correlation between conductivity and total dissolved solid in various type of water: a review, IOP Conf. Ser.: Earth Environ. Sci., 118 (2018) 012019.
[36] R. Lacatusu, C. Paltineanu, A. Vrînceanu, A.-R. Lacatusu, Influence of domestic activity on the quality of groundwater and surface water in the rural built-up area of the southern Romanian Danube Plain – a case study in the Glavacioc Catchment, Carpathian J. Earth Environ. Sci., 14 (2019) 323–334.
[37] A.M. Al-Shaibani, Hydrogeology and hydrochemistry of a shallow alluvial aquifer, western Saudi Arabia, Hydrogeol. J., 16 (2008) 155, doi: 10.1007/s10040-007-0220-y.
[38] N. Adimalla, S.K. Marsetty, P.P. Xu, Assessing groundwater quality and health risks of fluoride pollution in the Shasler Vagu (SV) watershed of Nalgonda, India, Hum. Ecol. Risk Assess.: An Int. J., 26 (2020) 1569–1588.
[39] E. Emmanuel, Y. Simon, O. Joseph, Characterization of hardness in the groundwater of port-au-prince. An overview on the health significance of magnesium in the drinking water, Aqua-LAC, 5 (2013) 35–43.
[40] S. Sumon, M.M. Arif Hasan, M. Zakir Hossain, A.K.M. Sadrul Islam, Mixed convection in an enclosure with different inlet and exit configurations, J. Appl. Fluid Mech., 1 (2008) 78–93.
[41] R. Mikutta, M. Kleber, K. Klaus, J. Reinhold, Review: organic matter removal from soils using hydrogen peroxide, sodium hypochlorite, and disodium peroxodisulfate, Soil Sci. Soc. Am. J., 69 (2005) 120–135.
[42] S. Lachache, M. Nabou, T. Merzougui, A. Amroune, Hydrochemistry and origin of principal major elements in the groundwater of the Béchar–Kénadsa basin in arid zone, South-West of Algeria, J. Water Land Dev., 36 (2018) 77–87.
[43] S. Abdesselam, A. Halitim, A. Jan, F. Trolard, G. Bourrié, Anthropogenic contamination of groundwater with nitrate in arid region: case study of southern Hodna (Algeria), Environ. Earth Sci., 70 (2013) 2129–2141.
[44] D. Kaown, K. Dong-Chan, M. Bernhard, L. Kang-Kun, Identification of nitrate and sulfate sources in groundwater using dual stable isotope approaches for an agricultural area with different land use (Chuncheon, mid-eastern Korea), Agric. Ecosyst. Environ., 132 (2009) 223–231.
[45] J.O. Odiyo, R. Makungo, T.G. Muhlarhi, The Impacts of Geochemistry and Agricultural Activities on Groundwater Quality in the Soutpansberg Fractured Aquifers, WIT Transactions on Ecology and the Environment Conference, WIT Press, Ashurst Lodge, 2014.
[46] Y. Shen, L. Huimin, Y. Dawen, S. Kanae, Effects of Agricultural Activities on Nitrate Contamination of Groundwater in a Yellow River Irrigated Region, Water Quality: Current Trends and Expected Climate Change Impacts (Proceedings of Symposium H04 Held During IUGG2011 in Melbourne, Australia, July 2011.
[47] Z. Atafar, A. Mesdaghinia, J. Nouri, M. Homaee, M. Yunesian, M. Ahmadi, A.H. Mahvi, Effect of fertilizer application on soil heavy metal concentration, Environ. Monit. Assess., 160 (2008) 83–89.

[48] T. Pugh Thomas, Calcium and magnesium in drinking-water: public health significance, Int. J. Environ. Stud., 67 (2010) 612–613.
[49] A. Potasznik, S. Sławomir, Magnesium and calcium concentrations in the surface water and bottom deposits of a river-lake system, J. Elementol., 20 (2015) 677–692.
[50] L. Bacciottini, A. Tanini, A. Falchetti, L. Masi, F. Franceschelli, B. Pampaloni, G. Giorgi, M.L. Brandi, Calcium bioavailability from a calcium-rich mineral water, with some observations on method, J. Clin. Gastroenterol., 38 (2004) 761–766.
[51] A.S. Arabi, I.I. Funtua, B.B.M. Dewu, M.L. Garba, S. Okoh, M.Y. Kwaya, M.T. Bolori, Assessment of calcium and magnesium concentrations in groundwater as supplements for sleep related ailments, J. Appl. Environ. Biol. Sci., 3 (2013) 29–35.
[52] P.Y. Li, J.H. Wu, H. Qian, Hydrochemical appraisal of groundwater quality for drinking and irrigation purposes and the major influencing factors: a case study in and around Hua County, China, Arabian J. Geosci., 9 (2016) 15, doi: 10.1007/s12517-015-2059-1.
[53] N. Khatri, S. Tyagi, Influences of natural and anthropogenic factors on surface and groundwater quality in rural and urban areas, Front. Life Sci., 8 (2015) 23–39.
[54] E. Morgado, P.L. Neves, Hypertension and Chronic Kidney Disease: Cause and Consequence – Therapeutic Considerations, H. Babaei, Ed., Antihypertensive Drugs, IntechOpen, 2012.
[55] N.N. Bukalo, E. Georges-Ivo, J.O. Odiyo, J.S. Ogola, Geochemistry of selected kaolins from Cameroon and Nigeria, Open Geosci., 9 (2017) 600–612.
[56] S.V. Sarath Prasanth, N.S. Magesh, K.V. Jitheshlal, N. Chandrasekar, K. Gangadhar, Evaluation of groundwater quality and its suitability for drinking and agricultural use in the coastal stretch of Alappuzha District, Kerala, India, Appl. Water Sci., 2 (2012) 165–175.
[57] S. Dhaka, N. Bhaskar, Assessment of groundwater quality in terms of water quality index and regression analysis of water quality parameters, J. Basic Appl. Eng. Res., 4 (2017) 339–342.
[58] M.R. El Tahlawi, M. Abu-El-Kassem, G.Y. Boghdady, R. Rabeiy, H.A. Saleem, Groundwater quality assessment to estimate its suitability for different uses in Assiut Governorate, Egypt, Int. J. Recent Technol. Eng., 3 (2011) 54–61.
[59] A.M. Piper, A graphic procedure in the geochemical interpretation of water-analyses, EOS, Transactions American Geophysical Union, 25 (1944) 914–928.
[60] S. Saha, A.H.M.S. Reza, M.K. Roy, Hydrochemical evaluation of groundwater quality of the Tista floodplain, Rangpur, Bangladesh, Appl. Water Sci., 9 (2019) 198, doi: 10.1007/s13201-019-1085-7.
[61] M. Sridharan, N. Senthil Nathan, Hydrochemical facies and ionic exchange in coastal aquifers of Puducherry Region, India: implications for seawater intrusion, Earth Syst. Environ., 1 (2017) 5, doi: 10.1007/s41748-017-0006-x.
[62] H.A.H. Musaed, A.M. Al-Bassam, F.K. Zaidi, H.J. Alfaifi, E. Ibrahim, Hydrochemical assessment of groundwater in mesozoic sedimentary aquifers in an arid region: a case study from Wadi Nisah in Central Saudi Arabia, Environ. Earth Sci., 79 (2020) 147, doi: 10.1007/s12665-020-8889-5.
[63] C.-W. Liu, K.-H. Lin, Y.-M. Kuo, Application of factor analysis in the assessment of groundwater quality in a blackfoot disease area in Taiwan, Sci. Total Environ., 313 (2003) 77–89.
[64] J. Mallick, K.S. Chander, M.K. AlMesfer, A. Kumar, R.A. Khan, S. Islam, A. Rahman, Hydro-geochemical assessment of groundwater quality in Aseer Region, Saudi Arabia, Water, 10 (2018) 1847, doi: 10.3390/w10121847.
[65] A.A. Al-Taani, A.T. Batayneh, S. Mogren, Y.H. Nazzal, H.A. Ghrefat, H. Zaman, E. Elawadi, Groundwater quality of coastal aquifer systems in the eastern coast of the Gulf of Aqaba, Saudi Arabia, J. Appl. Sci. Agric., 8 (2013) 768–778.
[66] A.J. Gibbs, G.A. Mcintyre, The diagram, a method for comparing sequences. Its use with amino acid and nucleotide sequences, Eur. J. Biochem., 16 (1970) 1–11.
[67] Y. Nazzal, A. Izrar, N.S.N. Al-Arifi, H. Ghrefat, F.K. Zaidi, M.M. El-Waheidi, A. Batayneh, T. Zumlot, A pragmatic approach to study the groundwater quality suitability for domestic and agricultural usage, Saq aquifer, northwest of Saudi Arabia, Environ. Monit. Assess., 186 (2014) 4655–4667.
[68] N. Subba Rao, Seasonal variation of groundwater quality in a part of Guntur District, Andhra Pradesh, India, Environ. Geol., 49 (2006) 413–429.
[69] M.H. El-Sayed, A.-H.M. El-Aassar, M.M.A. El-Fadl, A.M. Abd El-Gawad, Hydro-geochemistry and pollution problems in 10th of Ramadan City, East El-Delta, Egypt, J. Appl. Sci. Res., 8 (2012) 1959–1972.
[70] R. Barzegar, A.A. Moghaddam, E. Tziritis, Hydrogeochemical features of groundwater resources in Tabriz plain, Northwest of Iran, Appl. Water Sci., 7 (2017) 3997–4011.
[71] K. Lakhvinder, S.R. Madhuri, S. Sakshi, S. Bhavika, L. Renu, S. Gagandeep, Hydrogeochemical characterization of groundwater in alluvial plains of River Yamuna in Northern India: an insight of controlling processes, J. King Saud Univ. - Sci., 31 (2019) 1245–1253.
[72] D. Vasu, S.K. Singh, P. Tiwary, N. Sahu, S.K. Ray, P. Butte, V.P. Duraisami, Influence of geochemical processes on hydrochemistry and irrigation suitability of groundwater in part of semi-arid Deccan Plateau, India, Appl. Water Sci., 7 (2017) 3803–3815.
[73] R.A. Mir, J. Ghulam, Hydrogeochemical assessment of River Jhelum and its tributaries for domestic and irrigation purposes, Kashmir Valley, India, Curr. Sci., 109 (2015) 311–322.
[74] A. Modibo Sidibé, X.Y. Lin, K. Sidi, Assessing groundwater mineralization process, quality, and isotopic recharge origin in the Sahel Region in Africa, Water, 11 (2019) 789, doi: 10.3390/w11040789.
[75] N.T. Sigidi, J. Miller, A. Watson, C.E. Clarke, M. Butler, Geochemical and isotopic tracing of salt loads into the Ramsar Listed Verlorenvlei Estuarine Lake, South Africa, Procedia Earth Planet. Sci., 17 (2017) 909–912.
[76] A. Barkat, F. Bouaicha, O. Bouteraa, T. Mester, B. Ata, D. Balla, Z. Rahal, G. Szabó, Assessment of complex terminal groundwater aquifer for different use of Oued Souf Valley (Algeria) using multivariate statistical methods, geostatistical modeling, and water quality index, Water, 13 (2021) 1609, doi: 10.3390/w13111609.
[77] H. Schoeller, Qualitative Evaluation of Groundwater Resources, H. Schoeller, Ed., Methods and Techniques of Groundwater Investigation and Development, Water Resource Series No. 33, UNESCO, Paris, 1967, pp. 44–52.
[78] B. Lothenbach, Thermodynamic equilibrium calculations in cementitious systems, Mater. Struct., 43 (2010) 1413–1433.
[79] S. Chidambaram, U. Karmegam, P. Sasidhar, M.V. Prasanna, R. Manivannan, S. Arunachalam, S. Manikandan, P. Anandhan, Significance of saturation index of certain clay minerals in shallow coastal groundwater, in and around Kalpakkam, Tamil Nadu, India, J. Earth Syst. Sci., 120 (2011) 897–909.
[80] G. Bourrié, N. Salhi, R. Slimani, A. Douaoui, H.-A. Belhadj, M. Gihan, F. Trolard, Irrigation, Water and Soil Quality, G. Bourrié, Ed., Soils as a Key Component of the Critical Zone 4, ISTE Ltd and John Wiley & Sons, Inc., London, 2018, pp. 73–125.
[81] N. Aziane, A. Khaddari, M.I. Touhami, A. Zouahri, H. Nassali, M.S. Elyoubi, Evaluation of groundwater suitability for irrigation in the coastal aquifer of Mnasra (Gharb, Morocco), Mediterr. J. Chem., 10 (2020) 197, doi: 10.13171/mjc1020200222997nz.
[82] K.S. Rawat, S.K. Singh, S.K. Gautam, Assessment of groundwater quality for irrigation use: a peninsular case study, Appl. Water Sci., 8 (2018) 233, doi: 10.1007/s13201-018-0866-8.
[83] N. Aghazadeh, A.M. Asghar, Assessment of groundwater quality and its suitability for drinking and agricultural uses in the Oshnavieh Area, Northwest of Iran, J. Environ. Prot., 1 (2010) 30–40, doi: 10.4236/jep.2010.11005.
[84] S. Etteieb, S. Cherif, J. Tarhouni, Hydrochemical assessment of water quality for irrigation: a case study of the Medjerda River in Tunisia, Appl. Water Sci., 7 (2017) 469–480.
[85] L.A. Richard, Diagnosis and Improvement of Saline and Alkaline Soils, U.S. Salinity Laboratory, Agriculture Handbook No. 60 U.S. Dept. Agric., Supt. Documents, U.S. Government Printing Office Washington 25, D.C., 1954, 160 pages.

[86] O.P. Choudhary, K.K. Vilas, Soil Salinity and Sodicity, In: Soil Science: An introduction, New Delhi, 2018, pp. 53–384.
[87] Y.D. Ezlit, J.S. Rod, R.R. Steven, A Review of Salinity and Sodicity in Irrigation, Cooperative Research Centre for Irrigation Future, Irrigation Matters Series No. 01/10, 2010, p. 79.
[88] A.N.A. Hamdan, The assessment of the quality of water treatment plants effluent of Basrah City for Irrigation, Wasit J. Eng. Sci., 4 (2017), doi: 10.31185/ejuow.Vol4.Iss2.47.
[89] G. Santacruz de León, J. Alfredo Ramos Leal, J. Moran Ramírez, B. López Álvarez, E. Eliseo Santacruz de León, Quality indices of groundwater for agricultural use in the Soconusco, Chiapas, Mexico, Earth Sci. Res. J., 21 (2017) 117–127.
[90] A. Orhan, Doğu Trakya Bölgesi'nde Yeraltı Suyu Kalitesinin Araştırılması Amacıyla Coğrafi Bilgi Sistemi Yardımı ile Su Kalite İndeksi Uygulaması [Water Quality Index Application with the Help of Geographic Information System for the Investigation of Groundwater Quality in the Eastern Thrace Region], Jeol. Mühendisliği Derg., 2 (2016) 40.
[91] C. Güler, A. Mehmet, M. Alpaslan, C. Akbulut, Assessment of the impact of anthropogenic activities on the groundwater hydrology and chemistry in Tarsus Coastal Plain (Mersin, SE Turkey) using fuzzy clustering, multivariate statistics and GIS techniques, J. Hydrol., 414–415 (2012) 435–451.